25 May 2000

ELSEVIER

Optics Communications 179 (2000) 51–61

OPTICS COMMUNICATIONS

www.elsevier.com/locate/optcom

Superradiant amplification in an optically dense three-level cascade system [1]

Jamal T. Manassah [a,*], Irina Gladkova [b]

[a] *HMS Technology Corporation, PO Box 592, New York, NY 10028-0005, USA*
[b] *Department of Computer Science, City College of New York, New York, NY 10031, USA*

Received 4 November 1999; received in revised form 12 January 2000; accepted 12 January 2000

Abstract

We study superradiant amplification in a pressure-broadened three-level cascade system. The effects of the system initial coherence, degree of atomic inversion, and the length of the sample on the spatio-temporal distributions of the emitted fields from the upper and lower transitions are computed for a slab geometry. © 2000 Elsevier Science B.V. All rights reserved.

1. Introduction

The study of cooperative cascade emission from three-level atomic systems, $E_c > E_b > E_a$, was initially undertaken by Okada et al. [1–3]. In a series of further studies by Brownell and co-workers [4,5] and by ourselves [6,7], further experimental and numerical analysis of this problem were obtained for the case of low gas densities, i.e. the case where the atomic dephasing time is much longer than the superradiant time. In this paper, we generalize our previous work to incorporate theoretically the backward radiation from a slab geometry. In particular, we consider the exact problem dynamics when the gas is in the pressure-broadened regime [8,9]. Here, the medium is optically dense, i.e. the absorption length for a weak signal resonant with the lower transition and propagating in the gas system initially in the ground state is much shorter than the corresponding radiation wavelength. In this regime, the backward wave, from each layer inside the active medium, has to be properly incorporated at each step of the calculation. Furthermore, local field corrections [8,9] to the electromagnetic field, due to the difference between the microscopic Lorentz field and the macroscopic Maxwell field, in Bloch equations become important.

In this paper, we solve numerically the coupled integro-differential Maxwell–Bloch equations describing the electromagnetic radiation interaction with the pressure broadened three-level cascade medium. We do not assume, in Maxwell equations, the slowly varying envelope approximation in space, and we make, in Bloch equations, the distinction between the Maxwell and Lorentz fields. We compute for the cascade system, in the superradiant regime [10], the

* Corresponding author. Fax: +1-212-650-7185; e-mail: manassah@ees1s0.engr.ccny.cuny.edu

[1] Dedicated to Marlan O. Scully, in honor of his 60th birthday.

0030-4018/00/$ - see front matter
PII: S0030-4018(00)00491-0

fields resulting from the atomic upper and lower transition and the atomic density matrix elements spatio-temporal characteristics. We show that for an incoherently prepared system, the same kind of spatial symmetries in the fields distributions for the respective transition are present as found in two-level resonant systems, i.e. the pressure induced cavity field structure [11], which results from the interference between the forward and backward waves in the optically dense medium. Furthermore, we show that the bursts associated with the upper and lower transitions are sequential and the time delay between them is larger than the duration of the upper transition radiation burst. On the other hand, for a coherently prepared system, we show that the fields distributions, the transmitted and reflected fluxes, and the time-delay of the bursts from different components of the emitted radiation are substantially modified. In particular, we find: (i) the threshold for the onset of superradiance for the different radiation fields components; (ii) the regime for the upper transition forward radiation inhibition; (iii) the condition for yoked superradiance [5]; (iv) the superradiance overall efficiency; and (v) the extent of superbroadening for the respective spectral distributions. We obtain the detailed dynamics as function of the initial atomic population inversion and of the sample length.

Our analysis does not include the effects of the gas collision with the walls of the container, which, if kept hot to prevent condensation, can be neglected in the considered dense gas regime.

2. Maxwell–Bloch equations

The dynamics of the interaction of the electromagnetic field with the pressure-broadened three-level atoms system is described by the coupled Maxwell–Bloch equations. Neglecting the counter-rotating term in the Hamiltonian, Bloch equations, including the local field corrections, in the presence of the upper and the lower Maxwell fields, ϕ_{cb} and ϕ_{ba}, are given by:

$$\frac{\partial \rho_{aa}}{\partial \tau} = \Gamma_{ba}\,\rho_{bb} - \mathrm{i}\,\phi_{ba}\,\rho_{ba}^{*} + \mathrm{i}\,\phi_{ba}^{*}\,\rho_{ba} \tag{1}$$

$$\frac{\partial \rho_{bb}}{\partial \tau} = -\Gamma_{ba}\,\rho_{bb} + \Gamma_{cb}\,\rho_{cc} + \mathrm{i}\,\phi_{ba}\,\rho_{ba}^{*} - \mathrm{i}\,\phi_{ba}^{*}\,\rho_{ba} - \mathrm{i}\,\phi_{cb}\,\rho_{cb}^{*} + \mathrm{i}\,\phi_{cb}^{*}\,\rho_{cb} \tag{2}$$

$$\frac{\partial \rho_{cc}}{\partial \tau} = -\Gamma_{cb}\,\rho_{cc} + \mathrm{i}\,\phi_{cb}\,\rho_{cb}^{*} - \mathrm{i}\,\phi_{cb}^{*}\,\rho_{cb} \tag{3}$$

$$\frac{\partial \rho_{cb}}{\partial \tau} = -(\gamma_{cb} + \mathrm{i}\Delta_{cb})\,\rho_{cb} - \mathrm{i}\,\phi_{cb}^{L}(\rho_{cc} - \rho_{bb}) - \mathrm{i}\,\phi_{ba}^{L^{*}}\,\rho_{ca} \tag{4}$$

$$\frac{\partial \rho_{ba}}{\partial \tau} = -(\gamma_{ba} + \mathrm{i}\Delta_{ba})\,\rho_{ba} - \mathrm{i}\,\phi_{ba}^{L}(\rho_{bb} - \rho_{aa}) + \mathrm{i}\,\phi_{cb}^{L^{*}}\rho_{ca} \tag{5}$$

$$\frac{\partial \rho_{ca}}{\partial \tau} = -(\gamma_{ca} + \mathrm{i}\Delta_{cb} + \mathrm{i}\Delta_{ba})\,\rho_{ca} - \mathrm{i}\,\phi_{ba}^{L}\,\rho_{cb} + \mathrm{i}\,\phi_{cb}^{L}\,\rho_{ba} \tag{6}$$

where τ is the retarded time normalized to the classical Lorentzian shift ω_L, $\tau = \omega_L(t - z/v)$, $\omega_L = (Nd^2)/(6\hbar\varepsilon)$, N is the atomic number density, d is the dipole transition matrix element for the upper and lower transitions assumed here for simplicity to be equal, the deltas corresponding to the normalized detuning of the fields frequencies from that of the upper and lower transition resonance frequencies, the Γ's are the normalized natural decay constants, which will be neglected here, as compared to the γ's, the transverse decay times, due to collisions, the L superscripted fields are the Lorentz fields, and the normalized fields are the Rabi frequencies of the corresponding fields normalized to ω_L, i.e.

$$\phi_{cb} = \frac{dE_{cb}}{\hbar\,\omega_L}.$$

More specifically, and in order to study the present problem without the effects of additional complications due to the particular atomic structures details, we assume here the model where the atomic transition frequencies are separated by values much larger than the pressure broadened width, but infinitely smaller than the transition frequencies, and such that the spin structures of the upper and ground states are the same. Under such assumptions, we have:

$$\phi_{cb}^{L} = \phi_{cb} + \rho_{cb} \tag{7}$$

$$\phi_{ba}^{L} = \phi_{ba} + \rho_{ba} \tag{8}$$

$$\gamma_{cb} = a(\rho_{cc} + \rho_{bb}) \tag{9}$$

$$\gamma_{ba} = a(\rho_{bb} + \rho_{aa}) \tag{10}$$

$$\gamma_{ca} = 0. \tag{11}$$

Neglecting the effects of quantum modifications to the local field corrections, the constant a, for example, for a $J = 0 \to J = 1$ transition is equal to 1.7293. We shall use this value in subsequent calculations for illustrative purposes.

Assuming that the transit time in the slab (L/c) is much smaller than any of the problem time constants, and, as pointed earlier, that the pressure broadened width is much smaller than the transitions natural frequencies, the slowly-varying envelope approximation in time in Maxwell equation is justified. However, and as was also pointed earlier, the slowly-varying envelope approximation in space will not be made. This leads to the following form for Maxwell equations:

$$\frac{\partial^2 \phi_{cb}}{\partial \bar{z}^2} + \phi_{cb} = -3\rho_{cb} \tag{12}$$

$$\frac{\partial^2 \phi_{ba}}{\partial \bar{z}^2} + \phi_{ba} = -3\rho_{ba} \tag{13}$$

where $\bar{z} = kz$, and k is the wavenumber corresponding to the atomic transitions, taken here for simplicity to be the same for both the upper and lower transitions.

Using the Green's function for the Helmholtz equation, the above differential forms of Maxwell equations can be also written in an integral form [12,13]:

$$\phi_{cb}(\bar{z},\tau) = \phi_{cb}^{\text{in}}(\bar{z}=0,\tau)\exp(\mathrm{i}\bar{z}) + \mathrm{i}\frac{3}{2}\int_0^{\bar{L}} \mathrm{d}\bar{z}' \exp(\mathrm{i}|\bar{z}-\bar{z}'|)\rho_{cb}(\bar{z}',\tau) \tag{14}$$

$$\phi_{ba}(\bar{z},\tau) = \phi_{ba}^{\text{in}}(\bar{z}=0,\tau)\exp(\mathrm{i}\bar{z}) + \mathrm{i}\frac{3}{2}\int_0^{\bar{L}} \mathrm{d}\bar{z}' \exp(\mathrm{i}|\bar{z}-\bar{z}'|)\rho_{ba}(\bar{z}',\tau) \tag{15}$$

where the incoming fields are the external fields to the present atomic-field system. We shall use the above integral form of Maxwell wave-equation in subsequent numerical calculations.

3. Initializing the system dynamics

The problem of interest in this paper is the superradiance of a system excited through a two-photon process by a short pulse, i.e. the initial population of only the upper and ground states are nonzero, while that of the intermediate state is zero:

$$\rho_{cc}(\bar{z},\tau=0) = \chi$$

$$\rho_{bb}(\bar{z},\tau=0) = 0$$

$$\rho_{aa}(\bar{z},\tau=0) = 1-\chi. \tag{16}$$

Coherent excitation refers to the instance that the initial value for the off-diagonal matrix element ρ_{ca} is nonzero, i.e:

$$\rho_{ca}(\bar{z},\tau=0) = \sqrt{\chi(1-\chi)}\,\exp(2\mathrm{i}\bar{z}) \tag{17a}$$

while for incoherent excitation:

$$\rho_{ca}(\bar{z},\tau=0) = 0. \tag{17b}$$

To describe superradiant emission, we need to consider, in principle, the stochastic differential equations for the atom-field system. Instead, we simplify the problem here and replace the quantum fluctuations [14–19] of the Maxwell fields by external cw fields of magnitude equal to the square root of the expectation value of the quantum electrodynamics fields' fluctuations. This artifice will have the effect of initializing the spontaneous emission of the system (We use the value 10^{-9} for these fields). This approximation is valid when the number of photons is large, i.e. when we have classical fields, which is the case under consideration here.

4. Conservation laws

The above simplified system of coupled equations will be solved numerically through a similar algorithm to that described in Ref. [13]. Therefore, it is imperative that, at each step of the calculation, we

verify the accuracy of our results by comparing the results from the algorithm with those obtained from rigorous conservation integrals. Next, we shall derive these conservation laws:

1. Combining Eqs. (1)–(3), while neglecting the longitudinal relaxation times, we can derive the atomic number conservation law, specifically:

$$\frac{\partial}{\partial\tau}\left(\rho_{aa}(\bar{z},\tau)+\rho_{bb}(\bar{z},\tau)+\rho_{cc}(\bar{z},\tau)\right)=0$$

or

$$\rho_{aa}(\bar{z},\tau)+\rho_{bb}(\bar{z},\tau)+\rho_{cc}(\bar{z},\tau)=1. \tag{18}$$

2. Combining Eqs. (1)–(3) and Eqs. (12) and (13), and noting that:

$$\left.\frac{\partial\phi_{cb}(\bar{z},\tau)}{\partial\bar{z}}\right|_{\bar{z}=0}=-\mathrm{i}\,\phi_{cb}(\bar{z}=0,\tau) \tag{19a}$$

$$\left.\frac{\partial\phi_{cb}(\bar{z},\tau)}{\partial\bar{z}}\right|_{\bar{z}=\bar{L}}=\mathrm{i}\,\phi_{cb}(\bar{z}=\bar{L},\tau) \tag{19b}$$

with similar expressions for the $\phi_{ba}(\bar{z},\tau)$ field at the boundaries, we can derive the energy conservation laws, specifically:

$$\int_0^\infty\left[|\phi_{cb}(\bar{z}=0,\tau)|^2+|\phi_{cb}(\bar{z}=\bar{L},\tau)|^2\right]\mathrm{d}\tau = \frac{3}{2}\int_0^{\bar{L}}\left[\rho_{cc}(\bar{z},\tau=0)-\rho_{cc}(\bar{z},\tau=\infty)\right]\mathrm{d}\bar{z} \tag{20}$$

$$\int_0^\infty\left[|\phi_{ba}(\bar{z}=0,\tau)|^2+|\phi_{ba}(\bar{z}=\bar{L},\tau)|^2\right]\mathrm{d}\tau = \frac{3}{2}\int_0^{\bar{L}}\left[\rho_{aa}(\bar{z},\tau=0)-\rho_{aa}(\bar{z},\tau=\infty)\right]\mathrm{d}\bar{z}. \tag{21}$$

3. Combining the above equations with the initial conditions, specified in Section 3, we can deduce for the total flux from all the emitted radiation fields, the expression:

$$\int_0^\infty\left[|\phi_{cb}(\bar{z}=0,\tau)|^2+|\phi_{cb}(\bar{z}=\bar{L},\tau)|^2+|\phi_{ba}(\bar{z}=0,\tau)|^2+|\phi_{ba}(\bar{z}=\bar{L},\tau)|^2\right]\mathrm{d}\tau = 3\chi\bar{L}-\frac{3}{2}\int_0^{\bar{L}}\left[2\rho_{cc}(\bar{z},\tau=\infty)+\rho_{bb}(\bar{z},\tau=\infty)\right]\mathrm{d}\bar{z}. \tag{22}$$

Noting that the second term of the right hand side of this equation is always non-negative, then the upper limit to the total flux is $3\chi\bar{L}$. The efficiency of superradiance is defined as the ratio of the total flux from the reflected and transmitted parts of both fields to this upper limit.

In our numerical computations, the computational window size and the grid finesse are adjusted for each set of parameters such that Eq. (22) is, at each step, verified to an accuracy of better than 1%.

5. Results

The spatio-temporal distributions for the amplitudes of the upper and lower fields, for incoherent initial excitation of the system and for a sample length that admits the point $z=L/2$ as a center of spatial inversion symmetry in the case of the two-level system are plotted in Fig. 1. We note the following features:

(i) The invariance, also for the cascade three-level system, of the amplitudes of the fields with respect to a spatial inversion centered at $z=L/2$. This symmetry leads, of course, to equal transmitted and reflected signals for each of the fields. A situation comparable to the two-level dynamics.

(ii) The sequential nature of the superradiance bursts associated with the upper and lower transitions. Physically, the system emits the upper transition burst first, bringing the population of the intermediate state to a macroscopic value, then this intermediate state superradiates in turn to the ground state (a cascade process). The validity of this physical interpretation for the process can be verified by following the spatio-temporal behavior of ρ_{bb} (not shown here). Further confirmation for this process' simple mechanism is obtained by noting that the lower transition superradiance is absent when $\chi\leq 1/2$: In that case, $\rho_{aa}(\tau=0)\geq 1/2$ everywhere and the population of the intermediate state can never build up, even following complete upper level transition superradiance, to a value larger than $1/2$ thus inhibiting any lower transition superradiance since the system will then be an absorber at this frequency.

In Fig. 2, we plot the spatio-temporal distributions of the fields amplitudes for the same parameters as

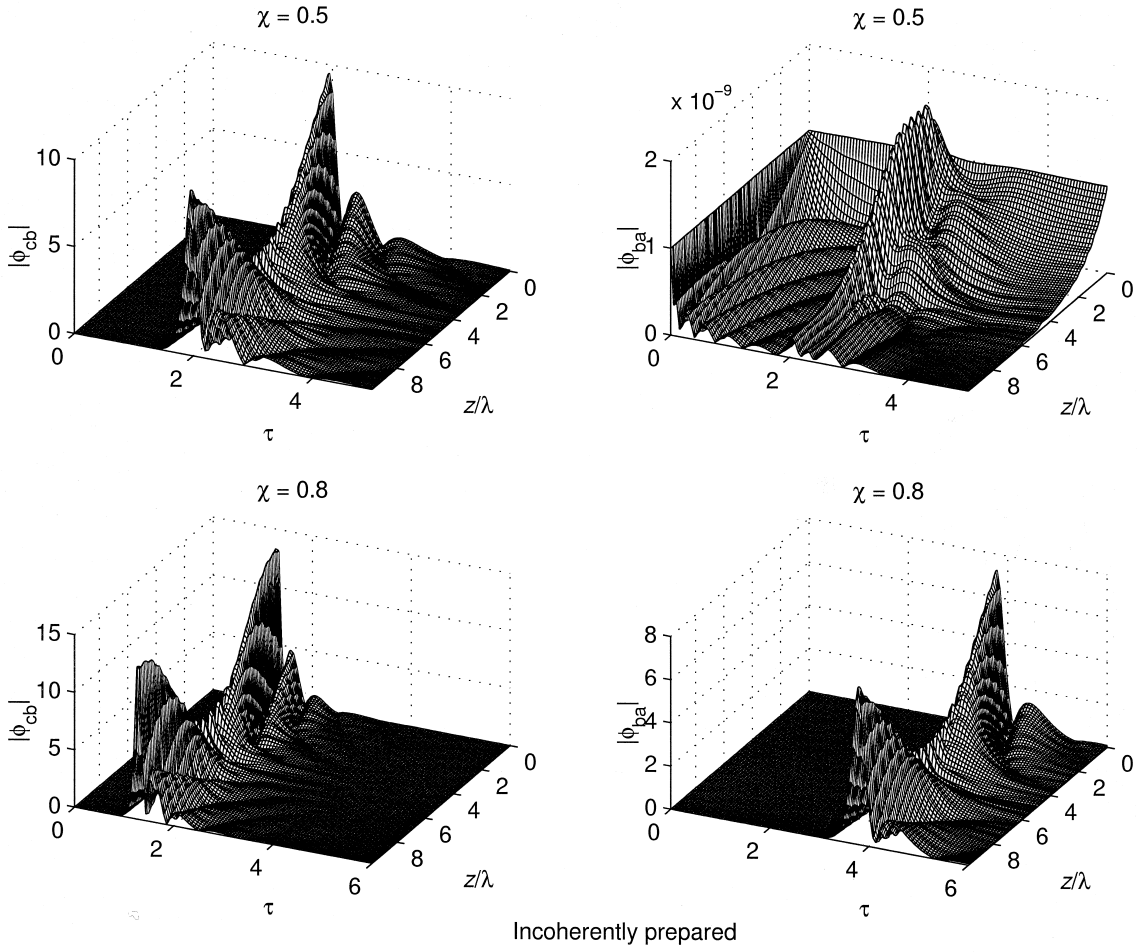

Fig. 1. The spatio-temporal dependence of the magnitude of the electric fields are plotted for an incoherently excited system $L = 9.75\lambda$.

in Fig. 1, but this time assuming that the system was initially coherently excited. In Fig. 3, we plot the time dependence of the amplitudes of reflected and transmitted fields for the cases shown in Figs. 1 and 2. We note the following:

(i) The spatio-temporal distributions of the upper and lower transitions fields are temporally overlapping, i.e. we have channels mixing. This can be understood by noting that the time-development of the off-diagonal density matrix elements ρ_{cb} and ρ_{ba}, the source terms for the ϕ_{cb} and ϕ_{ba} fields, have their dynamics now modified. In effect, their time development are now governed not only by the diagonal matrix elements (the terms that represent the population in the levels) but also by ρ_{ca} (see Eqs. (4) and (5)).

(ii) There is asymmetry between the transmitted and reflected fields for each of the transition. Furthermore, there is an inhibition in the upper transition transmission field, with the inhibition more pronounced for lower values of χ. This phenomenon has previously been predicted in Refs. [1–3], in the context of the linear theory as due to the preparation of the system in a two-photon coherence state.

(iii) The yoked superradiance between the upper lower and upper transmitted fields observed in Ref.

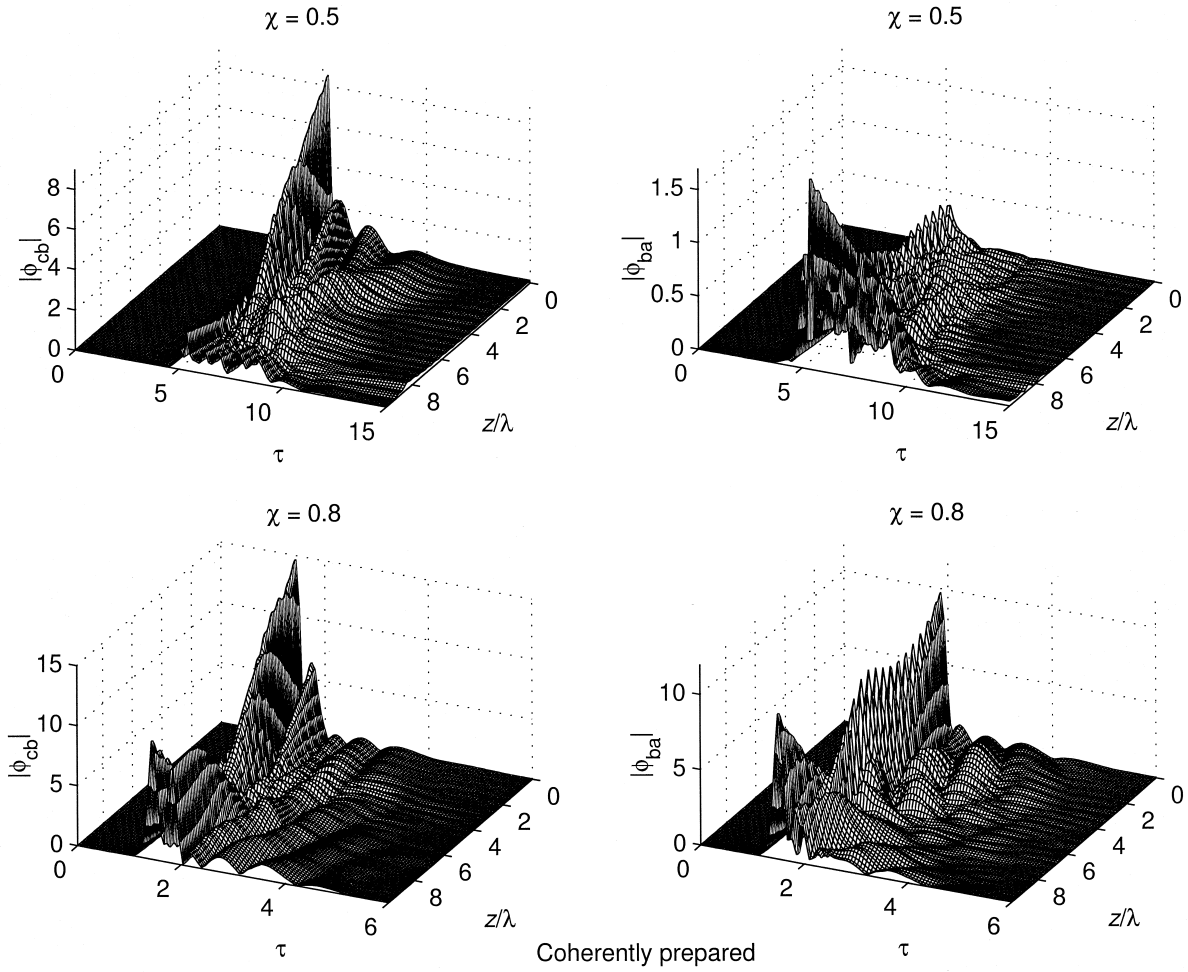

Fig. 2. The spatio-temporal dependence of the magnitude of the electric fields are plotted for a coherently excited system $L = 9.75\lambda$.

[5] is present. This phenomenon refers to the simultaneous emission of the upper and lower transmitted bursts, while leaving a lagging and smaller burst in the lower reflected channel. The dynamics of this phenomenon can be easily understood, in the linear regime, if we decompose ρ_{ca} into a forward and backward components. As the system begins its time development, the envelope of the forward component of ρ_{ca} is nonzero, while the envelope of the backward component averages to zero. The smaller amplitude for the lower reflected pulse which is also lagging is due to the depletion of the intermediate state population, resulting from the enhancement of the lower transmitted burst. This depletion leads to a delay and reduction of the source term responsible for the on-set of the reflected lower burst. Finally, it is worth noting that the yoked-superradiance process is manifest by the identical temporal profiles of the two transmitted fields, in the regime of the linear theory.

The normalized fluxes for the different radiation channels as function of the upper state initial population for both the incoherently and coherently prepared systems are plotted in Fig. 4. All the fluxes are

normalized to $3\chi\bar{L}$, i.e. the total normalized flux is < 1. We observe the following:

(i) The results of the linear theory previously mentioned are more detailed here.

(ii) The thresholds for the onset of superradiance vary, as noted earlier, with the initial state of coherence of the system.

(iii) The overall increase in the total superradiance efficiency for the coherently prepared system with the initial increase of χ. This can be understood by noting that the saturation effects observed in the incoherently prepared system and which is due to the buildup of the intermediate state population, will not be a constraint in the coherently prepared system,

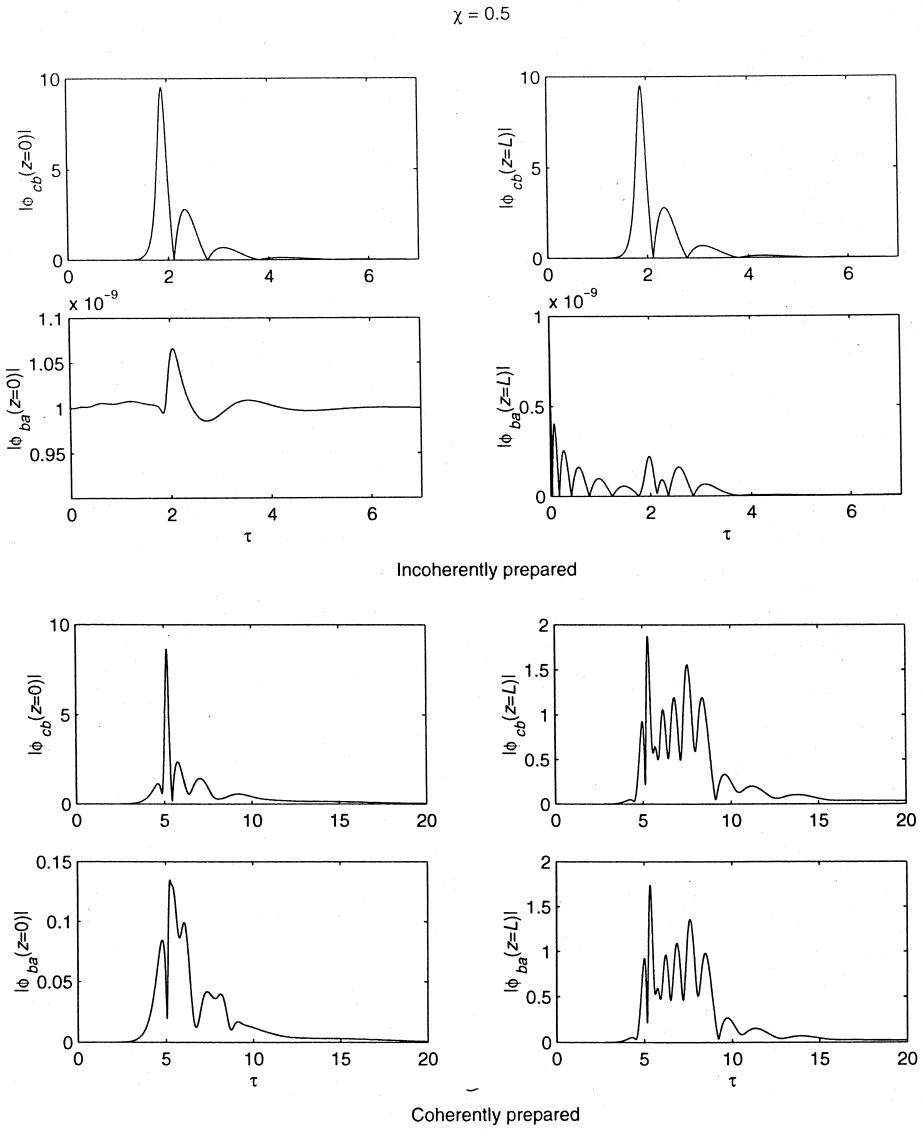

Fig. 3. The magnitude of the transmitted and reflected normalized fields, for the cases shown in Figs. 1 and 2, are plotted as function of the normalized time.

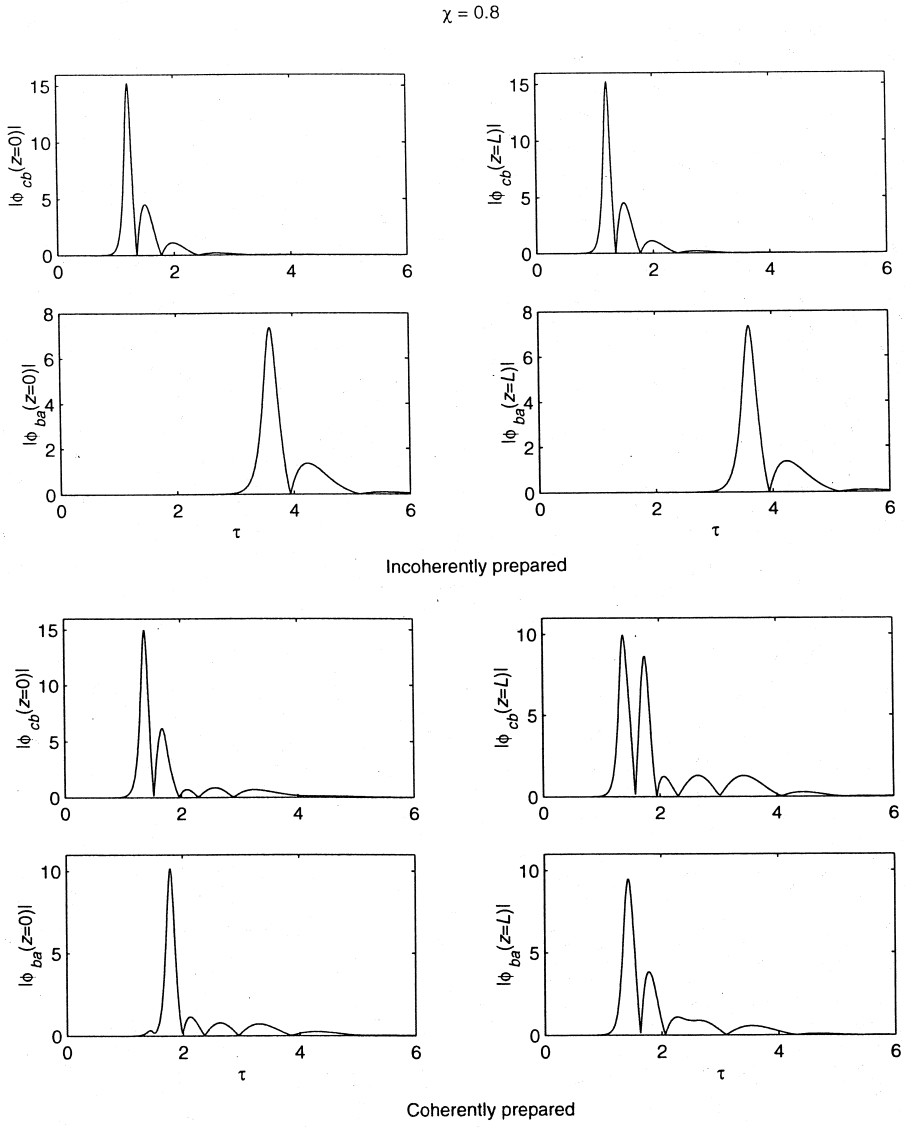

Fig. 3 (continued).

since the yoked-superradiance depletes the intermediate level population through the simultaneous emission corresponding to the transmitted lower transition. This process increases, in the coherently prepared system, the differential between the upper and intermediate levels population which of course leads to a more efficient emission process.

(iv) The transmitted and reflected fluxes for each channel converge to the same value when $\chi \to 1$, because for complete inversion there is no difference between coherently and incoherently prepared systems.

The normalized fluxes as function of the sample length for those values of the sample length, where

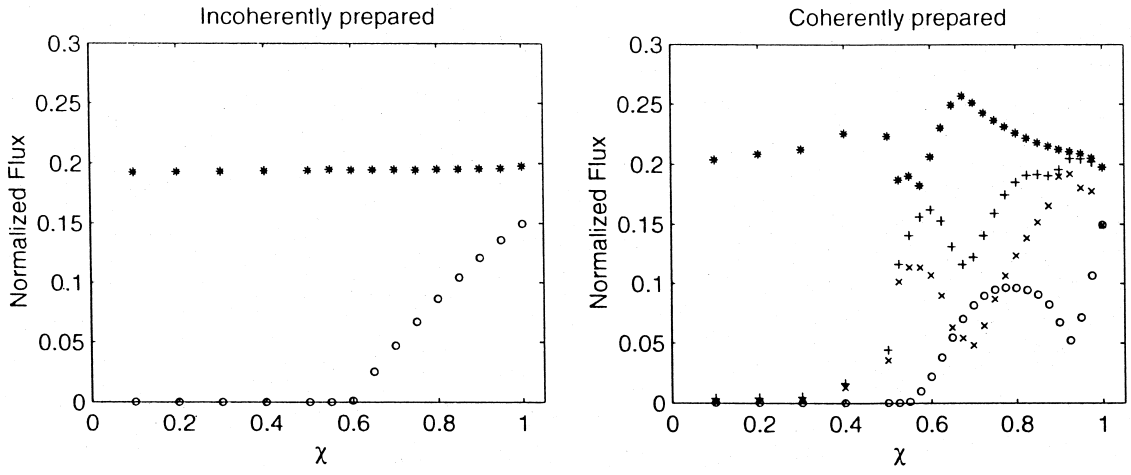

Fig. 4. The output fields normalized energy flux are plotted as function of the initial degree of upper-level excitation, for the different initial coherent state. $L = 9.75\lambda$. In these and the following graphs, we use the following symbols to denote the different fields components: * reflected cb; + transmitted cb; × transmitted ba; ∘ reflected ba.

for incoherent excitation, we have exact spatial symmetry with respect to the point $z = L/2$ (i.e. $= (n + 1/4)\lambda$ and $(n + 3/4)\lambda$) are plotted in Fig. 5. We note that:

(i) The normalized fluxes become substantial only for samples already longer than a wavelength.

(ii) The rate of increase of the total flux rises initially exponentially as function of the sample length, the linear or Beer's law regime, but then almost linearly in the deep nonlinear regime.

The normalized fluxes for a range of lengths corresponding in the two-level system to a transition domain (i.e. the domain defined by $(n + 1/4)\lambda < L < (n + 3/4)\lambda$) are plotted in Fig. 6. This is the domain over which the field amplitude changes from one parity eigenstate to another with respect to the

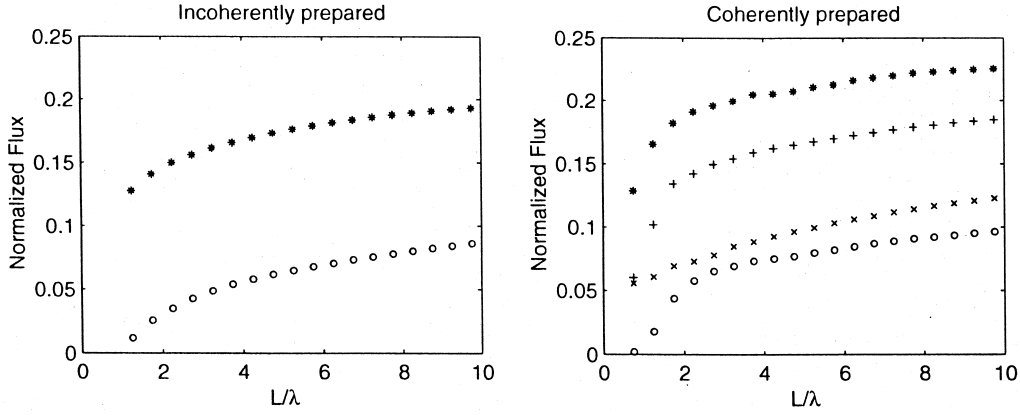

Fig. 5. The output fields normalized energy flux are plotted for $\chi = 0.8$, for values of the sample length at the discreet points $L = (n + 1/4)\lambda$ and $L = (n + 3/4)\lambda$.

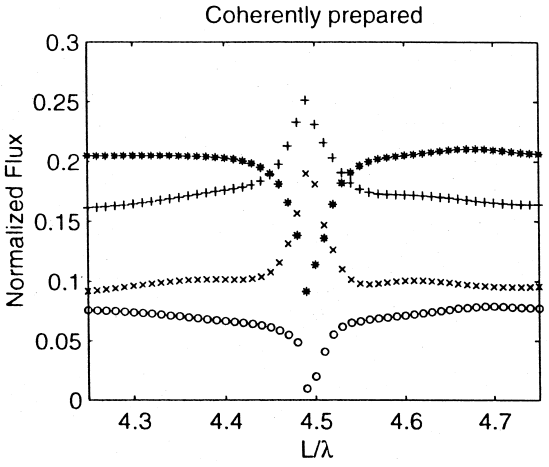

Fig. 6. The output fields normalized energy flux are plotted for $\chi = 0.8$ for length values in a transition domain.

operator corresponding to the spatial inversion around the mid-point of the sample. In this region, we have competition between the effects of the geometrical cavity and the pressure induced cavity. This competition leads for the case of the upper transition to the possibility of the enhancement of the transmitted radiation over the reflected radiation; while for the lower transition, the differential between the transmitted and the reflected radiation widens.

In Fig. 7, we plot the spectral distributions for the radiation in the different channels. We note the following:

(i) The asymmetry in the spectral distribution of the transmitted and reflected channels for each transition.

(ii) The additional confirmation for the yoked superradiance between the transmitted radiations from both transitions. In the linear regime, for every photon red (blue) shifted in the upper transition there will be one photon blue (red) shifted by the same amount in the lower transition, so as the total energy of both photons is constant and correspond to the energy difference between the upper and ground states. This translates in the mirror symmetry between the spectra of the two forward channels. It is to be observed that, as noted earlier, while the

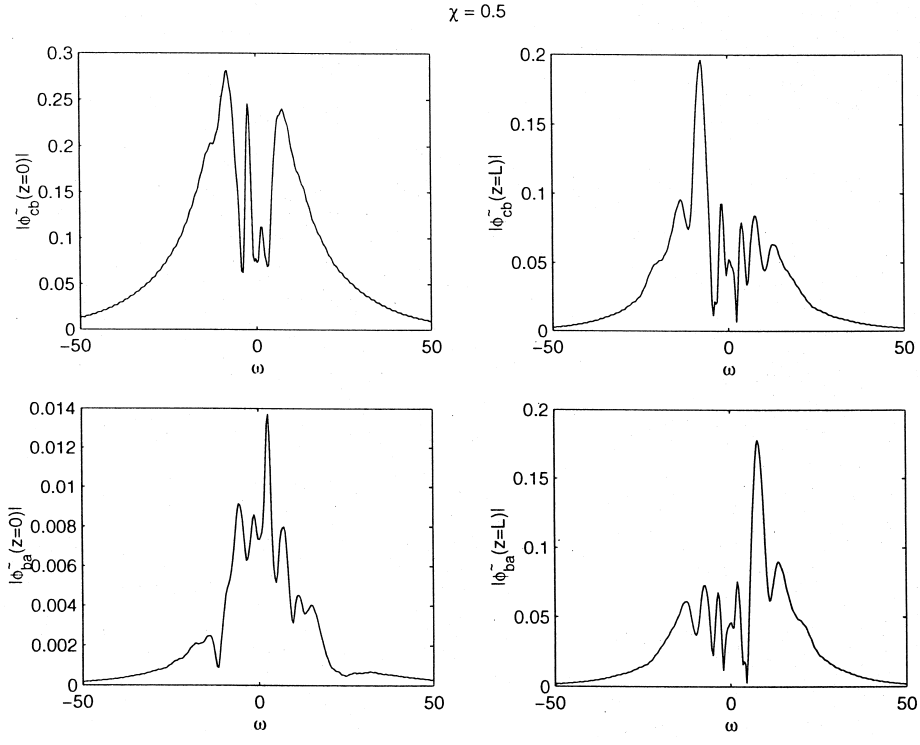

Fig. 7. The spectral distribution of the output fields are plotted for the different channels. $L = 9.75\lambda$ and $\chi = 0.5$.

amplitudes of the two fields have the same time-dependence, their phases are large in magnitude but opposite in sign.

(iii) The spectral distribution is superbroadened from the spectral width it would command from a measurement of the amplitude temporal distribution. Large phase-modulation (not shown here) is at the source of the observed large spectral width.

6. Conclusion

In this paper, we studied the superradiance from a ladder three-level pressure-broadened gas. We found that the state of initial coherence between the ground state and the upper state can dramatically modify the spatial and temporal dynamics of the superradiance in the different channels. The forward radiation inhibition from the upper transition, the yoked superradiance of the forward radiation for both transitions, the enhanced superradiance and different thresholds for superradiance in the different channels for a coherently prepared system were considered numerically in detail, and the validity of the associated physical pictures for these effects was verified.

References

[1] J. Okada, K. Ikeda, M. Matsuoka, Opt. Commun. 26 (1978) 189.
[2] J. Okada, K. Ikeda, M. Matsuoka, J. Phys. Soc. Jpn. 48 (1980) 1636.
[3] J. Okada, K. Ikeda, M. Matsuoka, J. Phys. Soc. Jpn. 48 (1980) 1646.
[4] H. Brownell, B. Gross, X. Lu, S.R. Hartmann, J.T. Manassah, Laser Phys. 3 (1993) 509.
[5] H. Brownell, X. Lu, S.R. Hartmann, Phys. Rev. Lett. 75 (1995) 3265.
[6] J.T. Manassah, B. Gross, Proc. SPIE 2098 (1994) 64.
[7] J.T. Manassah, B. Gross, Opt. Commun. 119 (1995) 663.
[8] R. Friedberg, S.R. Hartmann, J.T. Manassah, Phys. Rep. C 7 (1973) 101.
[9] J.T. Manassah, Phys. Rep. 101 (1983) 359.
[10] R.H. Dicke, Phys. Rev. 93 (1954) 99.
[11] J.T. Manassah, B. Gross, Opt. Commun. 143 (1997) 327.
[12] M.G. Benedict, V. Malyshev, E.D. Trifonov, A.I. Zaitsev, Phys. Rev. A 43 (1991) 3845.
[13] J.T. Manassah, B. Gross, Opt. Commun. 131 (1996) 408.
[14] J.C. MacGillivray, M.S. Feld, Phys. Rev. A 14 (1976) 1169.
[15] J.C. MacGillivray, M.S. Feld, Phys. Rev. A 23 (1981) 1334.
[16] R. Bonifacio, L.A. Lugiato, Phys. Rev. A 11 (1975) 1507.
[17] R. Bonifacio, L.A. Lugiato, Phys. Rev. A 12 (1975) 587.
[18] R. Glauber, F. Haake, Phys. Lett. A 68 (1978) 29.
[19] D. Polder, M.F.H. Schuurmans, Q.H.V. Vrehen, Phys. Rev. A 19 (1979) 1192.